A Genomic Screen for Modifiers of Tauopathy Identifies Puromycin-Sensitive Aminopeptidase as an Inhibitor of Tau-Induced Neurodegeneration

Stanislav L. Karsten,[1] Tzu-Kang Sang,[1,10]
Lauren T. Gehman,[1] Shreyasi Chatterjee,[1] Jiankai Liu,[1]
George M. Lawless,[1] Soma Sengupta,[5]
Robert W. Berry,[5] Justine Pomakian,[2] Hyun S. Oh,[6]
Cordula Schulz,[7] Koon-Sea Hui,[8]
Martina Wiedau-Pazos,[1] Harry V. Vinters,[2]
Lester I. Binder,[5] Daniel H. Geschwind,[1,3,4,9,*]
and George R. Jackson[1,3,9,*]
[1] Program in Neurogenetics
Department of Neurology
[2] Department of Pathology and Laboratory Medicine
[3] Center for Neurobehavioral Genetics
Semel Institute for Neuroscience and Human Behavior
[4] Department of Human Genetics
David Geffen School of Medicine at UCLA
Los Angeles, California 90095
[5] Department of Cell and Molecular Biology
Feinberg School of Medicine
Northwestern University
Chicago, Illinois 60611
[6] Department of Applied Statistics
Kyungwon University
Sungnam
South Korea
[7] Cold Spring Harbor Laboratories
Cold Spring Harbor, New York 11724
[8] The Nathan S. Kline Institute for Psychiatric Research
New York University School of Medicine
Orangeburg, New York 10962

Summary

Neurofibrillary tangles (NFT) containing tau are a hallmark of neurodegenerative diseases, including Alzheimer's disease (AD). NFT burden correlates with cognitive decline and neurodegeneration in AD. However, little is known about mechanisms that protect against tau-induced neurodegeneration. We used a cross species functional genomic approach to analyze gene expression in multiple brain regions in mouse, in parallel with validation in *Drosophila*, to identify tau modifiers, including the highly conserved protein puromycin-sensitive aminopeptidase (PSA/Npepps). PSA protected against tau-induced neurodegeneration in vivo, whereas PSA loss of function exacerbated neurodegeneration. We further show that human PSA directly proteolyzes tau in vitro. These data highlight the utility of using both evolutionarily distant species for genetic screening and functional assessment to identify modifiers of neurodegeneration. Further investigation is warranted in defining the role of PSA and other genes identified here as potential therapeutic targets in tauopathy.

*Correspondence: dhg@mednet.ucla.edu (D.H.G.); Grjackson@mednet.ucla.edu (G.R.J.)
[9] These authors codirected this work and are listed alphabetically.
[10] Present address: Institute of Biotechnology and Department of Life Science, National Tsing Hua University, Hsinchu-Taiwan, Republic of China.

Introduction

Pathological aggregation of the microtubule-associated protein tau is a defining feature of many neurodegenerative diseases collectively called tauopathies (Ingram and Spillantini, 2002; Lee et al., 2001). An essential role of tau in these disorders became evident with the discovery that tau mutations cause inherited forms of FTD with parkinsonism linked to chromosome 17 (FTDP-17) (Hutton et al., 1998; Ingram and Spillantini, 2002; Lee et al., 2001). The process of tau accumulation, paired helical filament (PHF) assembly, and aggregation is incompletely understood. While tau hyperphosphorylation clearly accelerates neurodegeneration (Grundke-Iqbal et al., 1986; Kosik and Shimura, 2005; Lee et al., 1991), the role of other posttranslational modifications, including proteolysis (Gamblin et al., 2003; Kosik and Shimura, 2005), ubiquitination (Bancher et al., 1991; Gong et al., 2005; Iqbal and Grundke-Iqbal, 1991), and nitration and glycosylation (Gong et al., 2005; Liu et al., 2002; Wang et al., 1996), as well as the function of the tau amino terminus in this process, remain unclear (Amadoro et al., 2004; Chen et al., 2004; Gamblin et al., 2003). A number of studies in vitro have identified potential proteases that are active against tau, including calpain, caspases, and thrombin (Arai et al., 2005; Gamblin et al., 2003; Mercken et al., 1995). However, their relationship to neurodegeneration observed in tauopathy is not known. Thus, identification of genetic factors that influence tau aggregation or degradation in vivo and modulate tau-induced neurodegeneration would have important implications for understanding tau-induced neurodegeneration and designing potential therapeutic interventions (Kosik et al., 2002; Kosik and Shimura, 2005; Lee et al., 2001; Price et al., 1998; Santacruz et al., 2005).

Here, we moved in a stepwise fashion from a large-scale microarray gene expression experiment to functional confirmation and identification of a pathway of tau processing that impacts neurodegeneration (Figure 1). We performed a genetic screen in mice expressing a common, dominant FTD-causing mutation in human tau, and used microarrays to identify gene expression changes in different brain regions. A subset of the gene expression changes was validated by both Northern blot analysis and in situ hybridization (Figure 2). We then performed functional validation in a well-characterized *Drosophila* model of tauopathy (Jackson et al., 2002), with particular focus on one of the genes, PSA (also known as Npepps), since it is a largely cytosolic aminopeptidase with very high expression in the CNS (McLellan et al., 1988; Tobler et al., 1997). PSA also is involved in the degradation of neuropeptide transmitters in vitro (Safavi and Hersh, 1995), but previously has not been demonstrated to affect tau. We found that PSA was upregulated in the cerebellum of mutant mice expressing the tau^{P301L} transgene, and we hypothesized that since its expression was changed in a region relatively resistant to neurodegeneration, it might represent part of a transcriptional compensatory
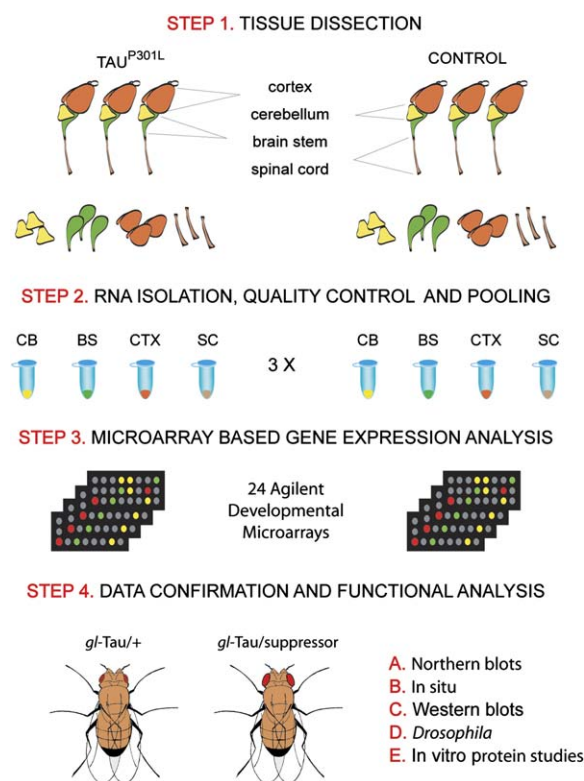
Figure 1. Schematic Depicting Experimental Procedures Used in the Study

Step 1: tissues were dissected from tau[P301L] and control nontransgenic animals. Step 2: RNA was isolated and combined into tissue- and litter-specific pools. RNA quality was verified prior to further experimentation. Step 3: microarray hybridizations and data analysis were performed resulting in the list of candidate genes. Step 4: identified gene expression changes were confirmed in independent animals. Expression of PSA was evaluated using in vitro and in vivo studies.

mechanism. We demonstrate that altering PSA expression has marked effects on tau-induced neurodegeneration in vivo in *Drosophila*. Reduced PSA expression increased neurodegeneration and tau aggregation, whereas overexpression of PSA inhibited neurodegeneration, concomitant with a reduction in tau immunoreactivity. These observations suggest that PSA can degrade tau in vivo via its aminopeptidase activity. We further confirmed that PSA catalyzes degradation of human tau in a cell-free system. Interestingly, Western blotting in human postmortem brain showed that PSA expression is higher in cerebellum than in frontal cortex in both FTD subjects and controls, suggesting a correlation between PSA levels and regional susceptibility to neurodegeneration that warrants further investigation.

Results

Regional Microarray Analysis of Tau[P301L] Mice

We conducted a comprehensive regional microarray analysis of transgenic mice expressing human tau[P301L] (Lewis et al., 2000), the most common human FTD mutation (Figure 1). These mice display many of the pathologic features of human tauopathies, including neurodegeneration in spinal cord and forebrain beginning

between 7 and 9 months of age (Ishizawa et al., 2003; Lewis et al., 2000; Lin et al., 2003). We compared gene expression in animals at 6 months of age, prior to the onset of a clinical phenotype or cell loss. At this stage, subtle biochemical abnormalities such as pathological tau phosphorylation can be identified in the absence of frank neurofibrillary tangles (NFT) and cell loss (Ishizawa et al., 2003; Lewis et al., 2000). This approach provided two advantages: first, it minimized potential confounds, such as changes in gene expression due to altered cell composition or cell loss, or factors secondary to neurodegeneration, such as malnutrition (Geschwind, 2000; Mirnics, 2001; Mirnics and Pevsner, 2004). Second, this approach made it more likely that we would identify biochemical changes during early phases of the neurodegenerative process that could potentially be more reversible than alterations identified during the later stages of disease. We also reasoned that some of the changes in gene expression occurring in brain regions relatively unaffected by neurodegeneration, such as the cerebellum, might reveal specific compensatory mechanisms that were involved in protecting that region. Thus, we performed a regional microarray analysis, comparing cerebral cortex, brainstem, cervical spinal cord, and cerebellum in transgenic and control nontransgenic animals using 24 Agilent Developmental mouse microarrays, which contain over 20,000 distinct probes. In each transgenic versus control comparison, three biological replicates, each representing at least three pooled littermates, were performed (Figure 1). A total of 31 probe sets that were differentially regulated between control and transgenic mice were identified using a combination of two analytic approaches; one was based on the false discovery rate, and the other was based on an empirically derived 99.5% confidence interval (Table 1). Half of the gene expression changes identified, which comprised 16 genes (11 enriched in tau[P301L] animals and five enriched in control animals) (Table 1), were found in the cerebellum.

We performed Northern blot analysis to provide quantitative confirmation of a randomly selected subset of six genes in independent nonlittermate animals of each genotype (Figure 2B). In all cases, the changes observed were significant (p < 0.01) and consistent with the microarray results. None of the changes were large, ranging between 1.5- and 2.5-fold, consistent with the mild phenotype at this stage. We also confirmed a subset of the changes by in situ hybridization in at least three independent nonlittermate animals of each genotype, confirming each of the differentially expressed genes tested (Figure 2). We specifically focused on confirming cerebellar expression changes, which were of particular interest as potential targets that could ameliorate tauopathy (e.g., Figures 2A and 2C; see below). Several genes were confirmed to be upregulated in cerebellum of mutant animals, including *Bcl2*, *Gtpbp3*, *Rab9*, and *Psa*, while others, such as *Vegfa* and *Mel13*, were downregulated in mutant animals (Figure 2; up in control).

Several genes that were differentially expressed in brain regions more involved with neurodegeneration in human FTD and the mouse model, such as those differentially expressed in the brainstem or spinal cord, had been implicated previously in neurodegenerative conditions such as amyotrophic lateral sclerosis (ALS)
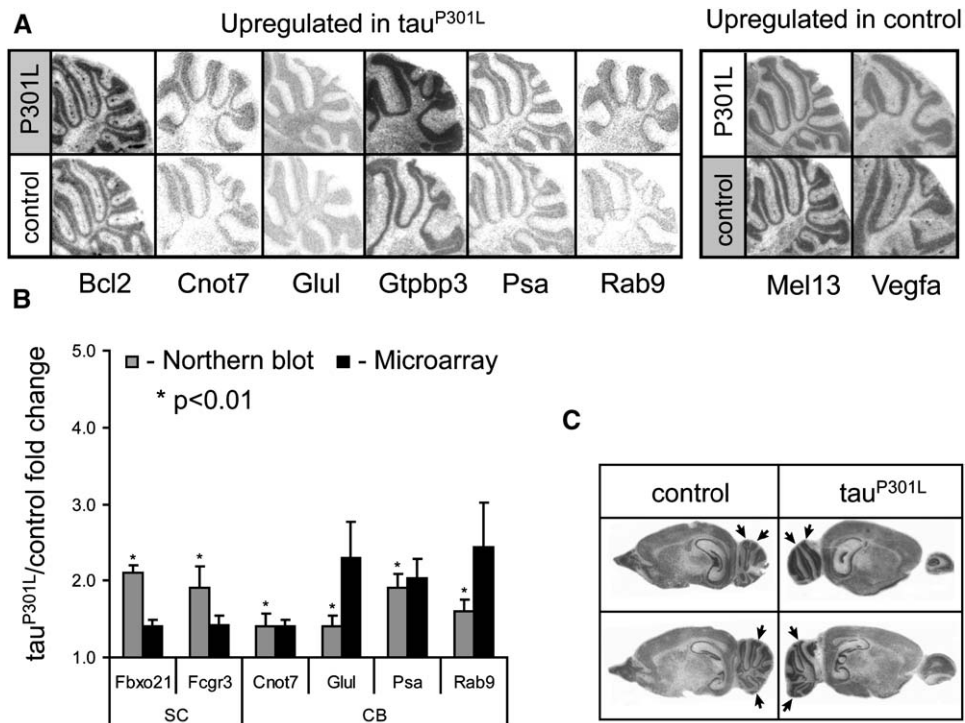
Figure 2. Confirmation of Microarray-Identified Genes Altered in Tau[P301L] Brain

(A) In situ expression patterns of about half of the genes up- (left panel) and downregulated (right panel) in tau[P301L] cerebellum. At least three nonlittermate animals of each genotype were used, and the images depicted were taken from sagittal sections of six month old brains hybridized to ^{35}S-labeled antisense cRNAs.

(B) Northern blot confirmation of microarray results in six genes of varying abundance using total RNA isolated from at least three independent nonlittermate animals of each genotype. Results are expressed as fold change for at least three animals each for tau[P301L] and control mice. The directions of expression patterns for all genes were in agreement with microarray data and were significant using two-tailed t tests ($p < 0.01$). Error bars, mean ± standard deviation.

(C) Sagittal sections show that *Psa* is specifically enriched in tau[P301L] cerebellum (arrows) relative to other regions, consistent with microarray and Northern data. SC, spinal cord; CB, cerebellum.

and AD. As an example, vesicle-associated membrane protein-associated protein B (*Vapb*) expression is altered in tau[P301L] brainstem, and mutations in the human *Vapb* gene result in spinal muscular atrophy and ALS (Nishimura et al., 2004). Motor neuron disease resembling ALS is observed in a significant subset of FTD patients, including those with the P301L mutation (Lee et al., 2001; Lomen-Hoerth, 2004). Thus, the identification of *Vapb* as a potential modifier of tauopathy provides a new potential molecular link between these conditions (Nishimura et al., 2004). Expression of insulin, insulin-like growth factors (IGFs), and insulin-like growth factor binding proteins (IGFBPs) is altered in many neurodegenerative diseases, including AD (Tham et al., 1993) and ALS (Wilczak et al., 2003), and *Igfbp2* was downregulated in tau[P301L] brainstem. Activation of complement is associated with an early response in AD (Shen and Meri, 2003), and complement component 1q γ polypeptide (*C1qg*) is significantly increased in tau[P301L] spinal cord, with a similar trend in the cortex and brainstem of tau[P301L] mice (Table 1).

In contrast, it was interesting to note that several genes enriched in tau[P301L] cerebellum were known to have protective properties in neurodegenerative conditions. As an example, *Bcl2* is an extensively studied outer mitochondrial membrane protein that has anti-apoptotic properties in a variety of systems, including the CNS (Gross et al., 1999), and *Lims1* is crucial for cell survival and protection of cells from apoptosis (Zhang et al., 2004). Other genes regulated in the cerebellum, including *Psa*, had not previously been implicated as potentially neuroprotective, and were interesting as they represented potentially novel modifiers of tau or tau-induced neurodegeneration (Figure 2). Since cerebellum is among the least affected brain regions in AD and FTD brain, as well as in tau[P301L] mice, and several identified changes involve genes with neuroprotective roles, we hypothesized that the differential regulation in some cases might reflect transcriptional compensation that protected against tau-induced neurodegeneration. Gain-of-function alleles of such genes would be expected to be suppressors of tauopathy, whereas loss-of-function of alleles would be expected to exacerbate tau-induced neurodegeneration.

PSA as a Suppressor of Tau-Induced Neurodegeneration in *Drosophila*

Misexpression of the longest 4-repeat isoform of human tau in *Drosophila* recapitulates pathological tau aggregation and neurodegeneration, including the formation of NFT and PHF when pathologically phosphorylated by a form of GSK-3β (Jackson et al., 2002). In this model,

Table 1. Genes Differentially Expressed between P301L Tau and Control Brains

GeneBank	Fold change tau^P301L/control				Method	p-value	Confirmation		Gene
	CX	BS	SP	CB			NB	In situ	
AK084095	2.4	-	-1.4	1.3	FDR	0.000			Atp6v0d1, ATPase, H+ transporting, V0 subunit D isoform 1
NM_029576	-1.5	-1.3	1.0	-	FC	-			Rab1b, member RAS oncogene family
AK220060	1.0	3.2	-1.1	1.0	FDR/FC	0.020			Eef1a1, eukaryotic translation elongation factor 1 alpha 1
NM_010097	1.0	1.9	1.0	-	FC	-			Sparcl1, SPARC-like 1
NM_015753	1.0	1.4	1.0	-	FC	-			Zfhx1b, zinc finger homeobox 1b
AK048417	1.1	1.8	1.2	-	FC	-			Vapb, vesicle-associated membrane protein, B
BC012724	1.0	-1.6	1.0	-	FDR	0.006			Igfbp2, insulin-like growth factor binding protein 2
NM_013697	1.8	-2.1	1.1	-	FDR	0.000			Ttr, transthyretin
NM_015744	1.1	-1.8	1.0	-	FC	-			Enpp2, ectonucleotide pyrophosphatase
NM_007574	1.2	1.4	1.5	1.1	FC	-			C1qg, complement component 1, q subcomponent, gamma
NM_010188	1.0	-	1.4	1.2	FC	-	+		Fcgr3, Fc receptor, IgG, low affinity III (CD16)
NM_009642	1.3	-	1.6	1.2	FC	-			Agtrap, Angiotensin II, type I receptor-associated protein
NM_145564	1.0	-	1.4	1.1	FC	-	+		Fbxo21, F-box only protein 21
AY130764	-1.1	-	-1.5	1.0	FC	-			Pkhd1, Polycystic kidney and hepatic disease 1
NM_011014	-1.1	-	-1.7	-1.3	FC	-	-		Oprs1, Opioid receptor, sigma 1
NM_009608	1.0	1.6	-1.1	2.4	FDR	0.000			Actc1, Actin, alpha, cardiac
NM_030255	1.1	1.5	-1.3	2.0	FDR	0.009	-		Apobec3, Apolipoprotein B editing complex 3
NM_009741	1.1	1.6	1.1	2.7	FDR	0.003		+	Bcl2, B-cell leukemia/lymphoma 2
NM_011135	1.3	1.4	1.4	1.4	FC	-	+	+	Cnot7, CCR4-NOT transcription complex, subunit 7
BC002136	1.0	1.3	-1.3	2.0	FDR	0.007			Coro1a, Coronin, actin binding protein 1A
NM_178379	1.1	1.6	-1.1	3.2	FDR	0.000		-	Cox10, Cytochrome c oxidase assembly protein
NM_008131	1.1	1.3	-1.1	2.3	FC	-	+	+	Glul, Glutamate-ammonia ligase
AY029613	1.0		-1.3	4.2	FDR	0.000		+	Gtpbp3, GTP binding protein 3
NM_008942	1.1	1.4	-1.1	2.0	FDR	0.007	+	+	Psa, Puromycin-sensitive aminopeptidase
NM_019773	1.1	2.1	-1.3	2.4	FDR	0.001	+	+	Rab9, member RAS oncogene family
BC067393	1.0	1.0	-1.2	1.5	FC	-			Lims1, LIM and senescent cell antigen-like domains 1
BC006583	1.0	-1.1	1.0	-2.3	FDR	0.005			RIKEN 4921511K06Rik
XM_126589	1.3	1.1	1.0	-2.9	FDR	0.000		+	Mel13, Melanoma nuclear protein 13
BC037129	1.1	1.0	1.1	-1.9	FDR	0.002			Gtpbp1, GTP binding protein 1
NM_020573	1.1	1.1	1.0	-2.0	FC	-			Osbpl1a, Oxysterol binding protein-like 1A
BC022642	1.0	-1.1	1.0	-2.8	FDR/FC	0.000		+	Vegfa, Vascular endothelial growth factor A

Gene names are listed (http://www.ncbi.nlm.nih.gov) alongside the Genbank Accession numbers representing the sequences used to construct the microarray probes. CX, cortex; BS, brainstem; SP, spinal cord; CB, cerebellum. The column designated "Method" indicates the criteria used for selection of regulated genes. FC, 1.4-fold change in all biological replicates. FDR, 0.05% false discovery rate. Genes confirmed with Northern blot (NB) analysis or in situ hybridizations are indicated in the penultimate column. Genes highlighted in yellow were in both mouse and fly.

tau expression produces a "rough" eye phenotype that reflects underlying neurodegeneration, as assessed by immunohistochemical staining in the larval eye disc, as well as neuronal loss and disorganization of the retina (Doglio et al., 2006; Jackson et al., 2002). This model is relevant to disease, as nearly half of the known FTD-causing mutations alter tau splicing by increasing the ratio of 4-repeat tau to 3-repeat tau (Hutton et al., 1998; Jackson et al., 2002; Lee et al., 2001). In addition, expression of mutant tau^P301L induces a similar phenotype (e.g., Figures 3 and 4). We therefore used this fly model as an initial screen to provide a cross-species functional assessment. Remarkably, one of the genes, PSA, was identified in an independent pilot screen for modifiers of tau-induced neurodegeneration using the first fifty lethal transposon insertions on the third chromosome, which was obtained from the Bloomington Stock Center (http://flystocks.bio.indiana.edu). We obtained additional lines of PSA and two other genes identified from the microarray screen, Vapb and Eef1a1, which also modified neurodegeneration caused by tau misexpression in the fly eye (Figures 3 and 4).

These observations provided an initial functional assessment and confirmation that the genes identified in the microarray screen in mouse play potential functional roles in modifying tau-induced neurodegeneration since the tau interactions in fly were consistent with dysregulation in tau^P301L mice (Table 1). A loss-of-function mutation of fly Vapb, DVAP-33A (Pennetta et al., 2002), suppressed neurodegeneration, consistent with its known role in human ALS (Nishimura et al., 2004) and the current microarray screen, in which it was upregulated in the brainstem, a vulnerable brain region (Figure 3B). Furthermore, a loss-of-function allele of EF1α48d, a fly homolog of Eef1a1, which was upregulated in the brainstem and thus postulated to confer tau vulnerability in the mouse, also suppressed the tau eye phenotype (Figure 3C), consistent with its potential role in sensitizing cells to apoptosis (Duttaroy et al., 1998). We also identified a transposon insertion strongly enhancing the tau eye phenotype that was in the 5′ UTR of Drosophila Psa (dPsa; Figure 4B). Similar results were obtained using a bona fide mutation (Schulz et al., 2001), consistent with the hypothesis based on microarray data
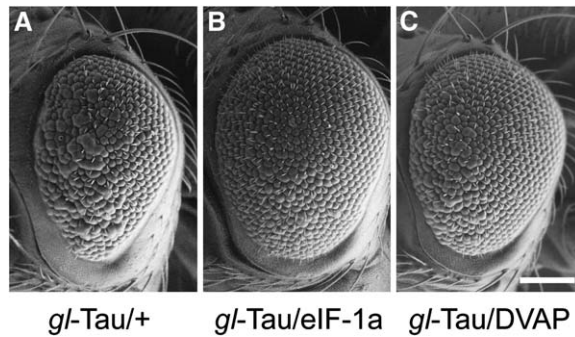
Figure 3. Suppression of the *gl*-Tau[WT] Phenotype by Mutations in *Eef1a1* and DVAP33A

(A–C) SEM images. The mild rough eye phenotype produced by one copy of *gl*-Tau (A) is suppressed in the presence of a piggyBac element allele of *Eef1a1* (B) or by a mutation of DVAP33A (C). Genotypes: (A), *w; gl*-Tau[WT]/+; (B), *w; gl*-Tau[WT]/+; eIF-1A[c04533]/+; (C), DVAP33A[448]/+; *gl*-Tau[WT]/+. Scale bar, 100 μm.

that overexpression of PSA would suppress, whereas loss of function of PSA would exacerbate, neurodegeneration (Figure 4B).

PSA Loss of Function Enhances Tau-Induced Neurodegeneration in *Drosophila*

Given the high expression of PSA in brain (McLellan et al., 1988; Tobler et al., 1997) and the recognition of the importance of the N terminus of tau in aggregation, coupled with a paucity of knowledge as to the proteolytic processing of tau (Gamblin et al., 2003; Lee et al., 2001), we focused our further efforts on PSA. To more directly assess the mechanism by which PSA activity affected tau-induced neurodegeneration in vivo, we examined whether PSA loss of function affected the *Drosophila* tau eye phenotype using several distinct lines. In contrast to the mild rough eye observed with tau alone (Figure 4A), tau expressed in combination with a transposon insertion in the 5′ UTR of dPSA produced a markedly enhanced phenotype (Figure 4B). Identical results were obtained using a large deletion of the PSA locus (data not shown). To assess whether PSA modifies the tau phenotype in a specific fashion, as opposed to having more general effects on neurodegenerative or cell death phenotypes, PSA loss- and gain-of-function lines were crossed with flies expressing a form of mutant huntingtin or the cell death gene *reaper.* No modification of either phenotype was observed (Figure 5), suggesting that the effect of PSA is not due to a generalized effect on cell death, but rather due to a more specific effect on tau.

PSA Expression Affects Tau Levels and Neurodegeneration

To explore the relationship of PSA to tau pathology further, we next examined tau expression and distribution in vivo in transgenic flies. Mild loss of photoreceptor neurons was produced by the human tau transgene, along with aberrant neuronal polarity, as described in detail previously (Jackson et al., 2002) (Figure 4D). Tau expression in a mutant *dPsa* background produced a more severe phenotype (Figure 4E). In contrast, low-level overexpression of dPSA reversed tau-induced
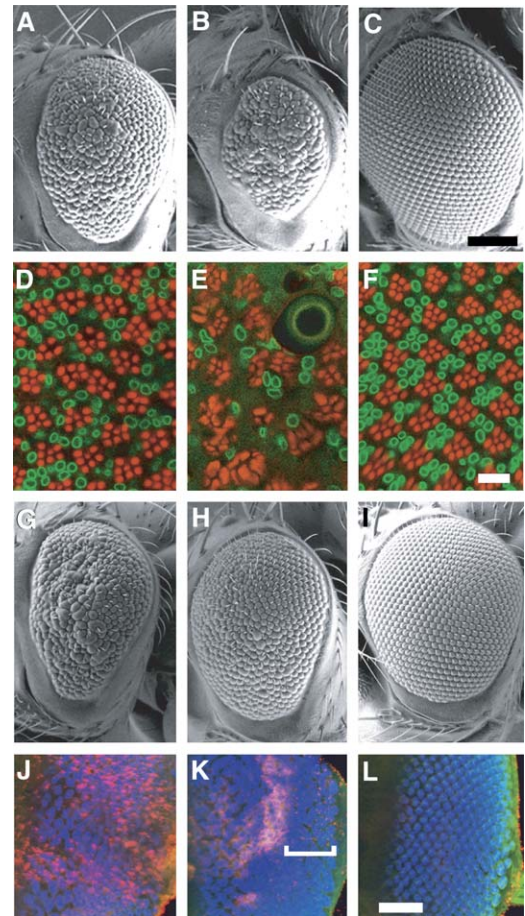

Figure 4. *Psa* Loss of Function Enhances, Whereas *Psa* Overexpression Suppresses, Tau-Induced Degeneration in the Eye

(A–C) SEM images showing enhancement of the *gl*-Tau[WT] phenotype (A) when expressed in *trans* to a P element allele of *Psa* (B), which has no phenotype on its own (C).

(D–F), Confocal images of adult retina stained with TRITC-phalloidin (red) and anti-lamin D_0 (green). Photoreceptor loss and disorganization caused by *gl*-Tau[WT] (D) are enhanced in *trans* to a PSA mutation (E) but suppressed when *Psa* is overexpressed at low levels using *hs*-PSA at 25°C.

(G–I) SEM images demonstrating suppression of the *gl*-Tau[WT] phenotype (G) using a direct fusion *gl*-*Psa* transgene (H), which has no eye phenotype on its own (I).

(J–L) Confocal images showing reduction of tau staining in third-instar larval eye disc by *Psa* coexpression. Blue, anti-Elav; red, T14; green, anti-*dPsa*. Anterior is shown toward the left. In the presence of *gl*-Tau[WT], tau expression (red) is apparent beginning at the morphogenetic furrow toward the left of the panel and is robust throughout the eye disc, even in posterior portions of the disc (J). When *gl*-*Psa* is coexpressed, however, posterior portions of the disc (bracket) show only residual tau (K). The *gl*-*Psa* transgene alone shows low levels of *Psa* staining (green), as expected (L). Scale bars, 100 μm ([A]–[C], [G]–[I]), 10 μm ([E]–[H]).

neurodegeneration and abnormalities of polarity (Figure 4F). We engineered new fly lines directly expressing tau under control of the *glass* (*gl*) promoter (Hay et al., 1995). The mild neurodegenerative phenotype induced by tau alone (Figure 4G) was suppressed by overexpression of dPSA (Figure 4H), whereas the phenotype of the *gl*-dPSA eye was normal (Figure 4I). We next examined whether dPSA overexpression affected tau levels using immunohistochemical analysis of larval eye discs.

Q120/+   Q120/Psa^LOF   Q120/Psa^GOF

rpr/+   rpr/Psa^LOF   rpr/Psa^GOF
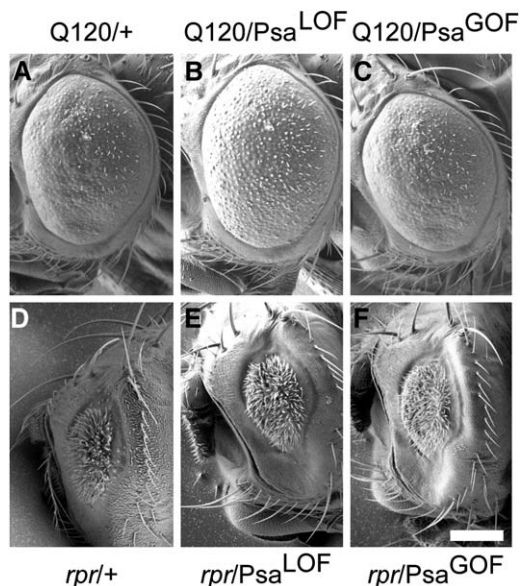
Figure 5. Manipulation of *Psa* Expression Has No Effect on Polygluta-mine or *reaper* Phenotypes

(A–C) SEM images showing phenotype of GMR-GAL4: 2X(UAS-htt-Q120^1-78) alone (A) or in *trans* to a *Psa* mutation (B) or a *hs*-PSA trans-gene driven at 25°C. (C). PSA loss of function or misexpression had no discernible effect on the polyglutamine phenotype.
(D–F) SEM images showing phenotype of GMR-*reaper* alone (D) or in *trans* to a PSA mutation (E) or a *hs*-PSA transgene (F). The *reaper* phenotype also was unaffected by alterations in *Psa* expression. Scale bar, 100 μm.

Staining of the eye disc enables comparison of cells that have just begun to coexpress tau and dPSA (near the morphogenetic furrow) with those that have been ex-pressing the two transgenes longer (toward the poste-rior of the disc). Although tau expression was apparent throughout the eye disc (Figure 4J), coexpression with dPSA resulted in loss of the majority of tau staining in posterior portions of the disc (bracket in Figure 4K). The *gl*-dPSA disc was normal, with low levels of dPSA detected in the weak lines selected for use in these stud-ies (Figure 4L). These data demonstrate that overex-pression of dPSA led to a substantial reduction of tau protein in parallel with its apparent neuroprotective ef-fect and suggest that this reduction in tau could underlie dPSA's modulation of tau-induced neurodegeneration.

PSA Robustly Suppresses the P301L Mutant Tau Phenotype

We next compared the effects of *dPsa* overexpression in eyes expressing tau^WT and tau^P301L in order to ascertain whether PSA was active against mutant tau, which is more pathogenic and prone to aggregation than wild-type tau (Arrasate et al., 1999; Rizzu et al., 1999). Whereas mild suppression of the *gl*-Tau^WT phenotype (Figure 6A) was observed with coexpression of *gl*-dPSA (Figure 6B), the *gl*-Tau^P301L phenotype (Figure 6C) was more dramatically suppressed by *gl*-dPSA (Figure 6D). Mild photoreceptor loss and aberrant polar-ity produced by *gl*-Tau^WT (Figure 6E) were largely sup-pressed by coexpression of *gl*-dPSA (Figure 6F). More-over, the apparent reduction of tau protein by dPSA overexpression that was apparent at earlier stages (Fig-
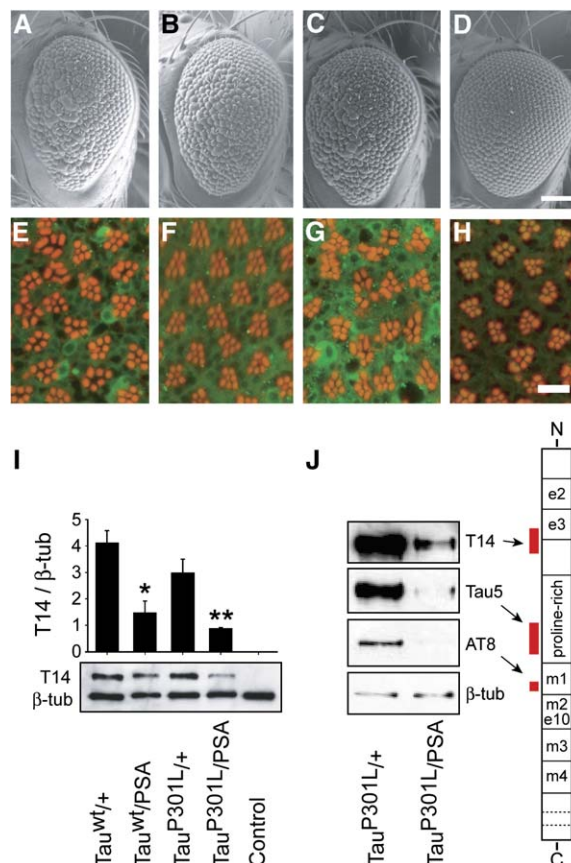
Figure 6. *Psa* Regulates Both Wild-Type and Mutant Tau Pheno-types

(A–D) SEM images comparing suppression of the *gl*-Tau^WT pheno-type (A) when coexpressed with *gl*-dPsa (B) and suppression of the *gl*-Tau^P301L phenotype (C) when coexpressed with *gl*-dPsa (D).
(E and F) Confocal images comparing suppression of the wild-type and mutant tau retinal phenotypes by coexpression of *Psa*. Red, TRITC-phalloidin; green, T14. The ommatidial polarity and mild rhabdomere loss associated with *gl*-Tau^WT (E) are suppressed when coexpressed with *gl*-dPsa (F); moreover, T14 staining is less abundant and more diffuse. The rhabdomere phenotypes associ-ated with *gl*-Tau^P301L (G) also are suppressed when coexpressed with *gl*-dPsa (H), and T14 immunoreactivity is markedly reduced. Scale bars, 100 μm ([A]–[D]); 10 μm ([E]–[H]).
(I) Western blot analysis demonstrating reduced steady state tau levels by coexpression of *dPsa*. Results shown are derived from densitometric analysis of three separate blots. Each bar represents mean ± SEM (n = 3). *$p < 0.05$; **$p < 0.001$, ANOVA + Bonferroni's comparison. A representative blot showing signals for T14 and β-tubulin is shown.
(J) Western blot analysis comparing effects of *Psa* on tau^P301L at a variety of different epitopes. Reduction of the amino-terminal T14 signal was accompanied by an epitope located within the more C-terminal proline-rich region (Tau5) as well as reduction of a confor-mation-dependent phosphoepitope (AT8).

ure 4) was also evident in the adult retina: the photore-ceptor abnormalities induced by *gl*-Tau^WT were accom-panied by both diffuse and focal accumulation of tau (Figure 6E), whereas coexpression with dPSA resulted in a more diffuse pattern of tau staining (Figure 6F). Sim-ilarly, dPSA suppression of the tau^P301L phenotype (Figure 6G) was accompanied by dramatic reductions in tau immunoreactivity (Figure 6H). We next compared the apparent reductions in both tau^WT and tau^P301L

levels observed using immunohistochemistry and Western blotting (Figures 6I and 6J). Representative Western blots showed reduced levels of both tau^WT and tau^P301L in flies coexpressing dPSA; these differences are observed with antibodies recognizing several distinct epitopes in tau (Figures 6I and 6J). Densitometric analysis revealed significant reductions in both tau^WT ($p < 0.05$) and tau^P301L ($p < 0.001$) levels by coexpression of *dPsa* (Figure 6I). These findings demonstrate that PSA is a previously unidentified modifier of neurotoxicity induced by tau misexpression or human disease-causing mutations and can diminish tau accumulation in vivo.

PSA Digests Tau In Vitro

The known function of PSA as an aminopeptidase, comprising over 90% of the aminopeptidase activity in the brain (McLellan et al., 1988), and the diminution of tau immunoreactivity in parallel with PSA overexpression observed here suggested that PSA acts directly on the amino terminus of tau via its peptidase activity. However, it was plausible that PSA had no direct interaction with tau, and was acting via cleavage of another intermediary. We therefore determined whether recombinant human PSA could cleave the longest isoform of human tau in a cell-free system. After 4 hr of incubation with PSA, full-length tau was partially diminished to ~65% of its original level, concomitant with the appearance of low-molecular weight, immunoreactive products likely representing the products of partial digestion (Figures 7A and 7B). Over the next 16 hr, this process continued, until after 18–20 hr of incubation, tau was digested completely by PSA. This process was inhibited by the specific PSA inhibitor puromycin and the more general aminopeptidase inhibitor bestatin (Figures 7C and 7D), providing confirmation that the observed tau degradation was due to the protease activity of PSA. Quantification of Western blots indicates that 90% of tau was digested by PSA, and that up to 90% of the tau was prevented from degradation by the inhibitors (Figure 7D). The observation that purified human PSA can directly cleave and significantly diminish human tau in vitro is consistent with data from *Drosophila* in vivo.

PSA Expression in Human Cortex and Cerebellum

We performed Western blotting using protein extracts from postmortem cortex and cerebellum of FTD cases (n = 6) and human controls (n = 6; see Table S1 in the Supplemental Data) to assess PSA protein levels in human brain. Remarkably, PSA expression was elevated 5-fold in the cerebellum as compared with frontal cortex in both controls and FTD cases (Figure 8A; normalized to β-tubulin). Comparison of PSA levels between FTD and controls showed a small but significant elevation of PSA in frontal cortex in FTD brains (see Figure S1 in the Supplemental Data). Immunohistochemistry confirmed previous observations that PSA is expressed primarily in neurons (Hui and Hui, 2003; Minnasch et al., 2003; Schonlein et al., 1994), as demonstrated by colocalization with the neuronal nuclear marker NeuN (Figures 8B and 8C). The qualitative immunohistochemical data support the more quantitative Western blot data, indicating that at the cellular level, PSA is increased in human cerebellum neurons relative to frontal cortical neurons (Figure 8).
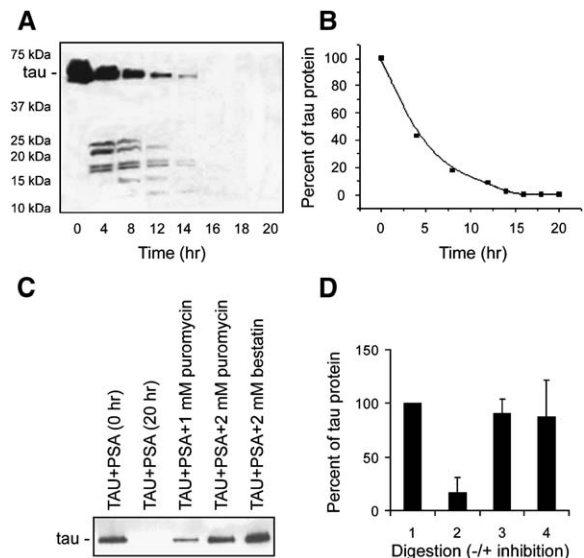

Figure 7. PSA Degrades Recombinant Tau Protein In Vitro

(A) Kinetics of PSA digestion of Tau as monitored by immunoblot analyses by Tau-46.1. The amount of protein loaded was 15 ng per lane. Tau was incubated with PSA for the indicated times and tau degradation was detected by Western blotting with mouse anti-tau antibody Tau-46.1.

(B) Densitometric analysis of the percentage of degradation of tau protein with time. The curve represents the densitometric averages of N-HT40 with time where tau protein incubated with PSA for 0 hr represents 100%. This figure shows that the approximate half-life of recombinant tau protein in the presence of PSA is about 4 to 5 hr.

(C) Western blot illustrating proteolysis of human tau by human PSA and inhibition by puromycin and bestatin. Blots (10 ng protein/lane) were probed with mouse anti-human Tau-7. Lanes 1 and 2, tau + PSA for 0 and 20 hr, respectively. Lanes 3 and 4, tau + PSA in the presence of 1 and 2 mM puromycin, respectively. Lane 5, tau + PSA in the presence of 2 mM bestatin.

(D) Quantitative analysis indicating the extent of digestion and inhibition. Bar graphs represent densitometric averages of three blots. Bar 1, tau + PSA for 0 hr represents 100%. Bar 2, percent tau digested following incubation with PSA for 20 hr. Bar 3, percentage of tau digested following incubation with PSA for 20 hr in the presence of 2 mM puromycin. Bar 4, percentage of tau digested following incubation with PSA for 20 hr in the presence of 2 mM bestatin. Blots were run in triplicate. Densitometric values represent the mean ± 1 SD.

Discussion

Here we use microarray analysis to identify genes whose expression is altered in conjunction with patterns of regional vulnerability in a mouse model of FTDP-17. We provide independent confirmation of a subset of these genes by Northern blotting and in situ hybridization and perform in vivo functional validation in another animal model, *Drosophila*. This work provides a clear proof of principle for validation of genetic screens using model systems and allows us to more firmly establish a functional role for one of the identified genes, *Psa*. Although *Psa* was known to be highly brain-enriched, to our knowledge, its role vis-a-vis tau degradation or modification of tau-induced neurodegeneration has not been characterized previously. We show that in the fly model, *dPsa* modulation of neurodegeneration is not likely to be a phenomenon related to a general or nonspecific suppression of cell death, as its overexpression or mutation

A

B
frontal cortex

C
cerebellum granular layer
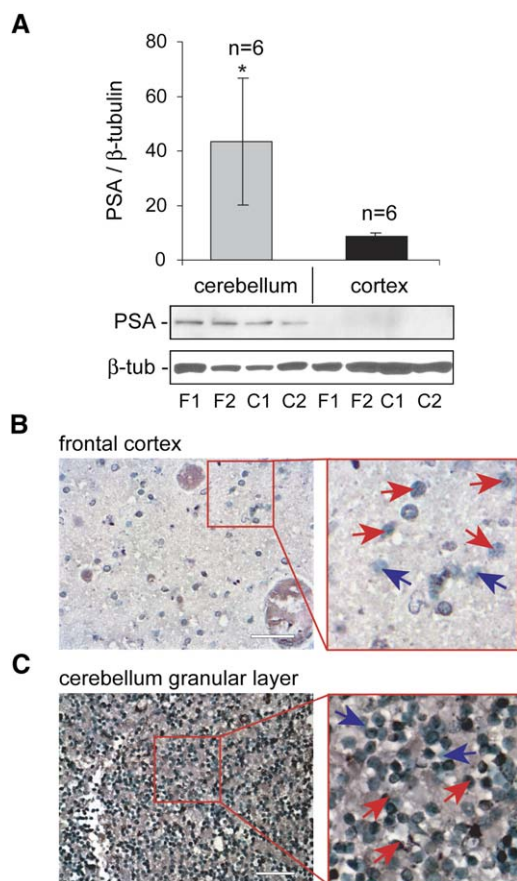
Figure 8. PSA is Elevated in Human Cerebellum as Compared with Frontal Cortex

(A) Western blot demonstrating reduced PSA levels in human cortex based on densitometric analysis of three separate blots. Each bar represents the mean ± SD (n = 6). PSA is elevated in cerebellum as compared with frontal cortex (single factor ANOVA; $\alpha < 0.05$; p = 0.004). Shown below the graph is a representative Western blot showing signals for PSA from cerebellum (first four lanes) and cortex (last four lanes). F indicates FTD specimens; C, control specimens. (B and C) Representative immunohistochemical images from cortex (B) and cerebellum (C) in the tissue microarray. Purple/blue, NeuN; brown, PSA. Scale bar, 100 μm.

has no observable effect on two other fly phenotypes. Furthermore, we show that human PSA can directly degrade human tau in vitro via its aminopeptidase activity, which is consistent with in vivo data in the fly showing that PSA overexpression coincides with loss of tau immunoreactivity.

Identification of genes likely to have functional relevance based on data derived from microarray experiments is often difficult, so independent confirmation and some degree of functional validation are needed to provide confidence in the significance of microarray results. However, confirming modifiers of late-onset neurodegenerative phenotypes in mice can be burdensome; hence, intermediate steps involving careful prioritization of potential targets are necessary. Although genetic modifiers of tauopathy in the fly have been identified (Shulman and Feany, 2003), functional validation of these modifiers in mammalian systems has not yet been reported. The combination of two distinct genetic

screens in model organisms described here provides an efficient way to approach discovery of novel disease modifiers. Data derived from in vivo studies with animal models and a cell-free system suggest that PSA may play a pivotal role in protection from tau-induced neurodegeneration, most likely by direct cleavage of tau. Tau levels are inversely correlated with PSA levels in vivo in the fly, and purified human PSA cleaves tau in a cell-free system. These data validate the use of *Drosophila* to screen for potential modifiers of disease, as this model organism provides an efficient and economical means for in vivo functional assessment of disease modifiers identified by microarray screening in mice.

In contrast to *Psa,* expression of *Vapb*, a vesicle trafficking protein, was elevated in tau[P301L] mouse brainstem, and thus this gene was considered as a potential enhancer or mediator of tau-induced neurodegeneration. This finding was notable as mutations in *Vapb* cause autosomal dominant motor neuron disease (Nishimura et al., 2004), supporting its potential involvement in neurodegeneration. It is also important to note that clinically apparent motor neuron disease is observed in 15% of patients with FTDP-17, and more have subclinical, pathological signs of motor neuron degeneration (Lee et al., 2001; Lomen-Hoerth, 2004). Here we show that *Vapb* mRNA was upregulated in a vulnerable region in tau[P301L] mice, whereas a loss-of-function mutation of the fly homolog suppressed the tau phenotype in the fly. Hence, *Vapb* provides a potential link between tauopathy and motor neuron disease in FTD that is worthy of further investigation.

Eef1a1, a ubiquitously expressed component of the translation initiation complex, was also identified in this study as being upregulated in the brainstem. Previous literature suggests that it may serve as a pro- or anti-apoptotic factor in different systems (Chen et al., 2000; Duttaroy et al., 1998; Talapatra et al., 2002). These data are consistent with the notion that elevated expression of *Eef1a1* is associated with susceptibility to tau-induced neurodegeneration. A loss-of-function allele of the *Drosophila* homolog strongly suppressed the tau phenotype, consistent with the notion that Eef1a1 is a prodegenerative factor.

Deciphering which of the observed changes in a microarray study are most relevant to the neurodegeneration observed in the human disease is a complex task (Geschwind, 2000; Small et al., 2005). Here we have applied a powerful filter to the data, focusing our downstream efforts primarily on expression changes in a region that, despite expressing high levels of the mutant gene of interest, exhibits no overt signs of neurodegeneration. In this manner, we were able to identify several genes with putative neuroprotective roles.

It has been suggested previously that amino terminal caspase-mediated cleavage of tau in vitro and in AD cases may be involved in NFT formation (Amadoro et al., 2004; Gamblin et al., 2003). Moreover, FTDP-17 mutations may render tau protein less susceptible to proteolysis, increasing the propensity of tau to form aggregates, consistent with the protective effects of PSA-mediated tau proteolysis. The observation here that *Psa* can also control tau toxicity in vivo supports the identification of this enzyme as a regulator of tau-induced neurodegeneration, perhaps analogous to the

role of proteolytic processing of other potentially toxic moieties, such as proteolytic processing of amyloid by presenilins or secretases (Hardy and Selkoe, 2002; Sisodia and St George-Hyslop, 2002).

A large body of evidence indicates that regulation of amyloid precursor protein (APP) and its proteolytic fragments plays a critical role in AD pathogenesis (Sisodia and St George-Hyslop, 2002). Similarly, it is clear from the human FTD-causing mutations that even relatively subtle changes in tau isoform levels can cause neurodegeneration (D'Souza and Schellenberg, 2005). Conversely, turning off an inducible mutant tau^{P301L} transgene after the onset of severe tau pathology in the mouse, thereby reducing mutant tau levels, can reverse the neurodegenerative process (Santacruz et al., 2005). Thus, it is tempting to speculate that factors that act to modulate tau levels or splicing, such as PSA, are candidates for playing a causal or contributory role in disease, and may represent potential targets for development of therapeutics. As an example, factors that lead to PSA downregulation in humans would be expected to increase tau, which in turn could contribute to disease susceptibility. The relatively high level of PSA expression, while correlative, within human cerebellar neurons (Figure 8A), which are less affected than cerebral cortex in AD and FTD, is consistent with this hypothesis. In addition, preliminary experiments assessing tau deposition and PSA levels by immunohistochemistry in postmortem cortical tissues from AD and FTD patients suggests an inverse relationship between PSA expression and tau deposition in neurons (data not shown). Similarly, we postulate that the trend toward a relative increase in PSA in postmortem FTD frontal cortex relative to controls (Figure S1) may reflect its higher level of expression in neurons surviving after a long course of disease. Neurodegeneration in FTD is known to primarily affect the superficial cortical laminae, so even within brain regions, different neurons are likely to show distinct patterns of vulnerability to neurodegeneration. The data described here provide a set of initial observations highlighting a potential role for PSA that warrant further analysis in other models and in human patient samples.

It is notable that PSA has been coimmunoprecipitated with APP (Schonlein et al., 1994) and colocalized around senile plaques in the cerebral cortex and hippocampus of AD brain (Minnasch et al., 2003). Although PSA does not directly alter APP levels in vitro, it is tempting to speculate that PSA could also provide a link between amyloid deposition and tau pathology observed in AD. While this and other questions relevant to the causal role of PSA in a spectrum of human diseases involving tau will be important to answer in future, its discovery as a protease potentially mediating tau degradation is an important step forward in understanding the pathogenesis of tauopathies and developing new therapeutic interventions in these fatal neurodegenerative diseases.

Experimental Procedures

Mice, Tissue Dissections, and RNA Isolation
Tau^{P301L} mice (Lewis et al., 2000) were housed in groups of up to four and kept on a 12 hr light/dark cycle at 22°C. Food pellets and water were available ad libitum. All animal protocols were in accordance with the NIH Guide for the Care and Use of Laboratory Animals and were approved by the UCLA animal studies committee. For gene expression experiments, the brains of 12 six-month-old tau^{P301L} and 12 nontransgenic males were dissected, separating the spinal cord, cortex, brainstem, and cerebellum (Figure 1A). Total RNA was extracted using acid phenol extraction (Trizol LS; GIBCO/BRL). The concentration and quality of RNA were determined using the Nanodrop spectrophotometer and confirmed on the Agilent bioanalyzer.

Microarray Data Analysis
All studies used the Agilent Developmental oligonucleotide microarray containing over 20,273 unique probes, representing 10,039 (49.5%) genes with a known full-length cDNA sequence (including 1584 RIKEN genes) and an additional 6289 (31.0%) ESTs. cDNA synthesis, cRNA labeling, hybridization, and scanning were performed according to the manufacturer's protocol (Agilent). To minimize sample variability caused by individual differences between animals and dissections, RNA from at least three male littermates of the same genotype was pooled for preparation of each region-specific pool (Figure 1). Experimental tau^{P301L} pools were compared to littermate nontransgenic control pools. The comparisons were performed in three different litters, therefore producing three independent biological replicates. In total, we obtained 24 expression profiles for cortex, spinal cord, brainstem, and cerebellum of tau^{P301L} and control animals.

The raw microarray data were analyzed in the R statistical package (http://lib.stat.cmu.edu/R/CRAN/index.html). The local background values were subtracted from the raw signal intensity values and transformed as log$_2$, which allows a natural interpretation of differential expression as fold changes and makes the intensity distribution more symmetric and the error variances more homogeneous. The log$_2$ intensities below the mean + 2.64 standard deviations of negative control intensities in each array were excluded from further analysis. The contrast-based cyclic lowess normalization method was used in the groups corresponding to a specific brain region (Bolstad et al., 2003). Normalizations were carried out in all distinct pairwise comparisons. Two different methods were used to identify differentially expressed genes. First, the local-pooled-error (LPE) method was used. The LPE method is known to be appropriate for a small number of replicated microarrays (Jain et al., 2003). The LPE was derived by evaluating the baseline error distribution in each brain region. Then, the median for each gene under the two comparison conditions was calculated. The LPE statistics for the median difference were calculated as

$$z = \frac{Med_1 - Med_2}{\sigma_{Pooled}},$$

where Med_i, $i = 1,2$ is the median intensity of the mutant and wild-type, respectively;

$$\sigma_{Pooled}^2 = \frac{\pi}{2}\left[\sigma_1^2(Med_1)/n_1 + \sigma_2^2(Med_2)/n_2\right],$$

where n_1 and n_2 are the number of replicates in the two conditions; and

$$\sigma_i^2(Med_i), i = 1, 2$$

is the estimate of the variance from each LPE baseline-error distribution at each Med_i. The LPE statistic Z follows an approximately normal distribution under the null hypothesis that the gene is not significantly different between two compared conditions. Thus, the raw p values were obtained for each gene (see Supplemental Data). The Benjamini and Hochberg false discovery rate was evaluated using a p value of 0.05 to adjust for multiple comparisons. In the second method, normalized expression levels were used to generate ratios of experimental/control signals. The genes with ≥ 0.5 or ≤ -0.5 ratios (1.4-fold change) through all replicates were selected as regulated (Table 1). This criterion was based on the 99.5% confidence interval derived from homotypic hybridizations (data not shown; as in Lobo et al., [2006]). Genes identified using at least one of the methods were considered to be regulated. For details regarding additional experimental design and methods, see MIAME report and http://geschwindlab.medsch.ucla.edu.

Northern Blot Analysis

For Northern blotting, total RNA was extracted from the cortex, cerebellum, brainstem, and spinal cord from at least three transgenic and three control male mice, all nonlittermates. Blots were prepared using 10 μg of total RNA and transferred to a Nytran SPC membrane (Schleicher & Schuell). Probe labeling, hybridization, and washes were done using the Strip-EZ protocol (Ambion). The Phosphor Imager system (Molecular Dynamics) was used to visualize and quantify the probe signals. For normalization controls, a β-actin probe was used.

In Situ Hybridization

In situ hybridizations were performed using six-month-old tau[P301L] and control animals as described previously (Geschwind et al., 2001). Slides contained at least three sagittal sections through entire brains of either control or tau[P301L] mice.

Drosophila Genetics and Phenotypic Analysis

A transposon insertion in the 5′ UTR of dPSA (*l(3)06226*) was identified initially as a tau enhancer in a pilot screen of lethal P element insertions on the third chromosome obtained from the Bloomington Stock Center (Bloomington Stock number 10158; http://flybase.org/.bin/fbidq.html?FBst0010158). (For listing of stocks see http://flystocks.bio.indiana.edu/Browse/insertions/GDP_all/pz-3.htm). Individual males for each P lethal line (maintained over balancer chromosomes) were crossed to females of the genotype y^1w^{1118}; *gl*-Tau[WT]-1.1 (Jackson et al., 2002); control crosses used y^1w^{1118} males. Eye phenotypes of progeny were scored under the dissecting microscope, and positive "hits" were evaluated further using scanning electron microscopy (SEM). Enhancers tend to decrease eye size and produce eyes with a more uniform rough appearance, (i.e., leading to fusion and loss of ommatidia), whereas suppressors increase size and tend to have the rough area confined to the most anterior portions of the eye. Findings using (*l(3)06226*) were subsequently confirmed using a characterized allele of PSA, PX49 (Schulz et al., 2001). Ubiquitous low-level overexpression of dPSA was accomplished using a heat shock (*hs*)-dPSA line and raising progeny at 25°C. To engineer the *gl*-dPSA line, dPSA was subcloned into pExpress-*gl*. Identity of the construct was confirmed by sequencing. Transgenic lines were obtained using standard techniques (Rubin and Spradling, 1982; Spradling and Rubin, 1982). As some *gl*-dPSA lines had abnormal phenotypes, we selected for lines with weak expression of dPSA in order to demonstrate clear genetic suppression. The DVAP33A mutant, which was produced using imprecise excision, was obtained from Hugo Bellen (Pennetta et al., 2002), and the piggyBac insertion (Thibault et al., 2004) in *Eef1a1* was obtained from the Bloomington Stock Center. The UAS-htt-Q120[1-78] construct was derived from GMR-htt-Q120[1-171] (Jackson et al., 1998).

Analysis of eye phenotypes using scanning electron microscopy was performed as described previously (Sang et al., 2005). Analysis of adult retinal phenotypes using whole-mount preparations in conjunction with laser scanning confocal microscopy was performed as described previously (Jackson et al., 2002; Sang et al., 2005). Samples were stained with TRITC-phalloidin (Sigma) and either anti-lamin D_0 (Smith and Fisher, 1989) (1:200) or T14 (Kosik et al., 1988) (1 μg/ml; Zymed), in conjunction with FITC-anti-mouse IgG. Immunohistochemical analysis of the larval eye disc was carried out using established procedures (Jackson et al., 2002; Sang et al., 2005). Samples were stained with T14 + TRITC-anti-mouse, anti-dPSA antiserum (1:100) + FITC-anti-rabbit, or anti-Elav (Robinow and White, 1988) (1:100) + Cy5-anti-rat IgG. The dPSA antiserum was raised against a peptide (CQRDREQLAIFFRDDQ) and generated commercially (Open Biosystems); it was found to react specifically with dPSA in immunohistochemistry and Western blots (data not shown). Secondary antibodies were from Jackson Immunoresearch.

Western Blotting

Crude protein extracts from postmortem frontal cortex and cerebellum of six FTD and six control brains were used (Table S1). The tissues were homogenized in hypotonic buffer and a protease inhibitor cocktail (Roche). Fly heads were homogenized in 10 mM Tris-HCl (pH 7.4) + 0.8 M NaCl + 1 mM EGTA (pH 8.0) + 10% sucrose and a protease inhibitor cocktail (Roche). Protein concentrations were determined by the Bradford assay (Bio-Rad) and samples containing approximately equal protein concentrations were loaded. Proteins were separated by SDS-PAGE using a 4%–20% Tris-HCl gel, transferred to nitrocellulose membranes, and incubated overnight at 4°C with goat anti-rat PSA (1:500), T14 (1:1000), AT8 (Biernat et al., 1992) (1:1000; Pierce), Tau5 (Carmel et al., 1996) (1:10,000), and/or anti-β-tubulin (1:1000, Accurate Science). Filters were treated with peroxidase-conjugated anti-goat (1:5000) or anti-mouse (1:2000) IgG and signal detected using chemiluminescence. Blots were scanned and quantitated using NIH ImageJ (http://rsb.info.nih.gov/ij/). Data were compiled from at least three separate experiments. Data were plotted using Sigmaplot, and two-way ANOVA with Bonferroni's post hoc comparison was carried out using Sigmastat.

Immunohistochemistry

The UCLA Department of Pathology provided formaldehyde-fixed and paraffin-embedded human postmortem brain tissue under UCLA human subject guidelines. Primary antibodies used in the study include goat anti-rat PSA serum (1:10) and mouse anti-neuronal nuclei (NeuN) monoclonal antibody (1:100) (Chemicon). Microwave boiling of deparaffinized sections in 0.015 M sodium citrate buffer (pH 6.0) for 12 min was employed as an antigen retrieval procedure. Sections were incubated overnight first with anti-NeuN, followed by incubation with the Vector ImmPRESS mouse reagent, and developed using the Vector Labs VIP kit. Sections were then reacted overnight with goat anti-rat PSA antiserum, followed by incubation with biotinylated horse anti-goat secondary antibodies (1:500) and development using the avidin-biotin complex kit (ABC; Vector Labs) and Vector DAB reagent. The slides were counterstained with Vector Methyl Green.

PSA Preparation and Enzymatic Activity

The cDNA corresponding to human PSA (hPSA) was generated by PCR from the Large Insert Human Brain cDNA library (Clontech) and ligated into the pET-41 Ek/LIC vector (Novagen) having an N-terminal glutathione S-transferase (GST) fusion tag. The pET-41-GST-hPSA construct was then transformed into *E. coli* BL-21-DE3* cells (Novagen). To reduce the extent of inclusion body formation, cells were grown at 18°C for 16 to 17 hr after induction by IPTG. Cells containing soluble PSA were harvested, resuspended in phosphate buffer (pH 7.3), and disrupted using a French press. After centrifugation, the supernatant was applied to a glutathione Sepharose column, and eluted fractions containing hPSA activity were pooled and further purified on a Superdex-200 column. The soluble, purified GST-PSA migrated largely as a single band on SDS-PAGE (data not shown). Enzymatic activity was assayed at 37°C using amino acid *p*-nitroanilides of Lys, Ala, Met, Leu, Val, and Pro on a Beckman DU 640 spectrophotometer employing a modified colorimetric assay (Constam et al., 1995).

Tau Preparation and Digestion with PSA

Expression and purification of full-length recombinant human tau protein was performed as described previously (Goedert et al., 1989). For time course analysis, digestion of 6XHis-Tau was carried out at 37°C in 10 mM Tris-HCl buffer (pH 7.4), containing 1 mM DTT at a molar ratio of 1:14.2 (PSA:tau). Aliquots were taken at 0, 4, 8, 12, 14, 16, 18, and 20 hr, and the reaction was terminated by the addition of Laemmli SDS sample buffer and boiling for 5 min. Samples were analyzed by electrophoresis on a 10%–20% SDS-PAGE gradient gel. Proteins were transferred to nitrocellulose and the membrane was immunostained with the C-terminal-specific antibody Tau-46.1 (Carmel et al., 1996) (1:50,000). Horseradish peroxidase (HRP)-conjugated secondary antibody (Vector Laboratories) and enhanced chemiluminescence (Amersham Biosciences) were used to visualize the bands.

For inhibitor experiments, digestion of tau was carried out at 37°C for 20 hr in 10 mM Tris-HCl buffer (pH 7.4) containing 1 mM DTT at a molar ratio of 1:14.2 (PSA:tau). Proteins were electrophoresed and transferred to nitrocellulose membranes, which were incubated with Tau-7, which recognizes the C-terminal portion of tau. Inhibition experiments were carried out using puromycin (Sigma), a specific inhibitor of PSA, or a general inhibitor of aminopeptidases, bestatin (Sigma). The inhibitors were incubated for 5 to 10 min at room

temperature prior to the addition of tau protein and digestion as described above.

References

Amadoro, G., Serafino, A.L., Barbato, C., Ciotti, M.T., Sacco, A., Calissano, P., and Canu, N. (2004). Role of N-terminal tau domain integrity on the survival of cerebellar granule neurons. Cell Death Differ. 11, 217–230.

Arai, T., Guo, J.P., and McGeer, P.L. (2005). Proteolysis of non-phosphorylated and phosphorylated tau by thrombin. J. Biol. Chem. 280, 5145–5153.

Arrasate, M., Perez, M., Armas-Portela, R., and Avila, J. (1999). Polymerization of tau peptides into fibrillar structures. The effect of FTDP-17 mutations. FEBS Lett. 446, 199–202.

Bancher, C., Grundke-Iqbal, I., Iqbal, K., Fried, V.A., Smith, H.T., and Wisniewski, H.M. (1991). Abnormal phosphorylation of tau precedes ubiquitination in neurofibrillary pathology of Alzheimer disease. Brain Res. 539, 11–18.

Biernat, J., Mandelkow, E.M., Schroter, C., Lichtenberg-Kraag, B., Steiner, B., Berling, B., Meyer, H., Mercken, M., Vandermeeren, A., Goedert, M., et al. (1992). The switch of tau protein to an Alzheimer-like state includes the phosphorylation of two serine-proline motifs upstream of the microtubule binding region. EMBO J. 11, 1593–1597.

Bolstad, B.M., Irizarry, R.A., Astrand, M., and Speed, T.P. (2003). A comparison of normalization methods for high density oligonucleotide array data based on variance and bias. Bioinformatics 19, 185–193.

Carmel, G., Mager, E.M., Binder, L.I., and Kuret, J. (1996). The structural basis of monoclonal antibody Alz50's selectivity for Alzheimer's disease pathology. J. Biol. Chem. 271, 32789–32795.

Chen, E., Proestou, G., Bourbeau, D., and Wang, E. (2000). Rapid upregulation of peptide elongation factor EF-1alpha protein levels is an immediate early event during oxidative stress-induced apoptosis. Exp. Cell Res. 259, 140–148.

Chen, F., David, D., Ferrari, A., and Gotz, J. (2004). Posttranslational modifications of tau–role in human tauopathies and modeling in transgenic animals. Curr. Drug Targets 5, 503–515.

Constam, D.B., Tobler, A.R., Rensing-Ehl, A., Kemler, I., Hersh, L.B., and Fontana, A. (1995). Puromycin-sensitive aminopeptidase. Sequence analysis, expression, and functional characterization. J. Biol. Chem. 270, 26931–26939.

Doglio, L.E., Kanwar, R., Jackson, G.R., Perez, M., Avila, J., Dingwall, C., Dotti, C.G., Fortini, M.E., and Feiguin, F. (2006). gamma-cleavage-independent functions of presenilin, nicastrin, and Aph-1 regulate cell-junction organization and prevent tau toxicity in vivo. Neuron 50, 359–375.

D'Souza, I., and Schellenberg, G.D. (2005). Regulation of tau isoform expression and dementia. Biochim. Biophys. Acta. 1739, 104–115.

Duttaroy, A., Bourbeau, D., Wang, X.L., and Wang, E. (1998). Apoptosis rate can be accelerated or decelerated by overexpression or reduction of the level of elongation factor-1 alpha. Exp. Cell Res. 238, 168–176.

Gamblin, T.C., Chen, F., Zambrano, A., Abraha, A., Lagalwar, S., Guillozet, A.L., Lu, M., Fu, Y., Garcia-Sierra, F., LaPointe, N., et al. (2003). Caspase cleavage of tau: linking amyloid and neurofibrillary tangles in Alzheimer's disease. Proc. Natl. Acad. Sci. USA 100, 10032–10037.

Geschwind, D.H. (2000). Mice, microarrays, and the genetic diversity of the brain. Proc. Natl. Acad. Sci. USA 97, 10676–10678.

Geschwind, D.H., Ou, J., Easterday, M.C., Dougherty, J.D., Jackson, R.L., Chen, Z., Antoine, H., Terskikh, A., Weissman, I.L., Nelson, S.F., and Kornblum, H.I. (2001). A genetic analysis of neural progenitor differentiation. Neuron 29, 325–339.

Goedert, M., Spillantini, M.G., Potier, M.C., Ulrich, J., and Crowther, R.A. (1989). Cloning and sequencing of the cDNA encoding an isoform of microtubule-associated protein tau containing four tandem repeats: differential expression of tau protein mRNAs in human brain. EMBO J. 8, 393–399.

Gong, C.X., Liu, F., Grundke-Iqbal, I., and Iqbal, K. (2005). Posttranslational modifications of tau protein in Alzheimer's disease. J. Neural Transm. 112, 813–838.

Gross, A., McDonnell, J.M., and Korsmeyer, S.J. (1999). BCL-2 family members and the mitochondria in apoptosis. Genes Dev. 13, 1899–1911.

Grundke-Iqbal, I., Iqbal, K., Tung, Y.C., Quinlan, M., Wisniewski, H.M., and Binder, L.I. (1986). Abnormal phosphorylation of the microtubule-associated protein tau (tau) in Alzheimer cytoskeletal pathology. Proc. Natl. Acad. Sci. USA 83, 4913–4917.

Hardy, J., and Selkoe, D.J. (2002). The amyloid hypothesis of Alzheimer's disease: progress and problems on the road to therapeutics. Science 297, 353–356.

Hay, B.A., Wassarman, D.A., and Rubin, G.M. (1995). Drosophila homologs of baculovirus inhibitor of apoptosis proteins function to block cell death. Cell 83, 1253–1262.

Hui, M., and Hui, K.S. (2003). Neuron-specific aminopeptidase and puromycin-sensitive aminopeptidase in rat brain development. Neurochem. Res. 28, 855–860.

Hutton, M., Lendon, C.L., Rizzu, P., Baker, M., Froelich, S., Houlden, H., Pickering-Brown, S., Chakraverty, S., Isaacs, A., Grover, A., et al. (1998). Association of missense and 5′-splice-site mutations in tau with the inherited dementia FTDP-17. Nature 393, 702–705.

Ingram, E.M., and Spillantini, M.G. (2002). Tau gene mutations: dissecting the pathogenesis of FTDP-17. Trends Mol. Med. 8, 555–562.

Iqbal, K., and Grundke-Iqbal, I. (1991). Ubiquitination and abnormal phosphorylation of paired helical filaments in Alzheimer's disease. Mol. Neurobiol. 5, 399–410.

Ishizawa, T., Sahara, N., Ishiguro, K., Kersh, J., McGowan, E., Lewis, J., Hutton, M., Dickson, D.W., and Yen, S.H. (2003). Co-localization of glycogen synthase kinase-3 with neurofibrillary tangles and granulovacuolar degeneration in transgenic mice. Am. J. Pathol. 163, 1057–1067.

Jackson, G.R., Salecker, I., Dong, X., Yao, X., Arnheim, N., Faber, P.W., MacDonald, M.E., and Zipursky, S.L. (1998). Polyglutamine-expanded human huntingtin transgenes induce degeneration of Drosophila photoreceptor neurons. Neuron 21, 633–642.

Jackson, G.R., Wiedau-Pazos, M., Sang, T.K., Wagle, N., Brown, C.A., Massachi, S., and Geschwind, D.H. (2002). Human wild-type tau interacts with wingless pathway components and produces neurofibrillary pathology in Drosophila. Neuron 34, 509–519.

Jain, N., Thatte, J., Braciale, T., Ley, K., O'Connell, M., and Lee, J.K. (2003). Local-pooled-error test for identifying differentially expressed genes with a small number of replicated microarrays. Bioinformatics 19, 1945–1951.

Kosik, K.S., and Shimura, H. (2005). Phosphorylated tau and the neurodegenerative foldopathies. Biochim. Biophys. Acta. 1739, 298–310.

Kosik, K.S., Orecchio, L.D., Binder, L., Trojanowski, J.Q., Lee, V.M., and Lee, G. (1988). Epitopes that span the tau molecule are shared with paired helical filaments. Neuron 1, 817–825.

Kosik, K.S., Ahn, J., Stein, R., and Yeh, L.A. (2002). Discovery of compounds that will prevent tau pathology. J. Mol. Neurosci. *19*, 261–266.

Lee, V.M., Balin, B.J., Otvos, L., Jr., and Trojanowski, J.Q. (1991). A68: a major subunit of paired helical filaments and derivatized forms of normal Tau. Science *251*, 675–678.

Lee, V.M., Goedert, M., and Trojanowski, J.Q. (2001). Neurodegenerative tauopathies. Annu. Rev. Neurosci. *24*, 1121–1159.

Lewis, J., McGowan, E., Rockwood, J., Melrose, H., Nacharaju, P., Van Slegtenhorst, M., Gwinn-Hardy, K., Paul Murphy, M., Baker, M., Yu, X., et al. (2000). Neurofibrillary tangles, amyotrophy and progressive motor disturbance in mice expressing mutant (P301L) tau protein. Nat. Genet. *25*, 402–405.

Lin, W.L., Lewis, J., Yen, S.H., Hutton, M., and Dickson, D.W. (2003). Ultrastructural neuronal pathology in transgenic mice expressing mutant (P301L) human tau. J. Neurocytol. *32*, 1091–1105.

Liu, F., Zaidi, T., Iqbal, K., Grundke-Iqbal, I., Merkle, R.K., and Gong, C.X. (2002). Role of glycosylation in hyperphosphorylation of tau in Alzheimer's disease. FEBS Lett. *512*, 101–106.

Lobo, M.K., Karsten, S.L., Gray, M., Geschwind, D.H., and Yang, X.W. (2006). FACS-array profiling of striatal projection neuron subtypes in juvenile and adult mouse brains. Nat. Neurosci. *9*, 443–452.

Lomen-Hoerth, C. (2004). Characterization of amyotrophic lateral sclerosis and frontotemporal dementia. Dement. Geriatr. Cogn. Disord. *17*, 337–341.

McLellan, S., Dyer, S.H., Rodriguez, G., and Hersh, L.B. (1988). Studies on the tissue distribution of the puromycin-sensitive enkephalin-degrading aminopeptidases. J. Neurochem. *51*, 1552–1559.

Mercken, M., Grynspan, F., and Nixon, R.A. (1995). Differential sensitivity to proteolysis by brain calpain of adult human tau, fetal human tau and PHF-tau. FEBS Lett. *368*, 10–14.

Minnasch, P., Yamamoto, Y., Ohkubo, I., and Nishi, K. (2003). Demonstration of puromycin-sensitive alanyl aminopeptidase in Alzheimer disease brain. Leg. Med. (Tokyo) *5* (Suppl 1), S285–S287.

Mirnics, K. (2001). Microarrays in brain research: the good, the bad and the ugly. Nat. Rev. Neurosci. *2*, 444–447.

Mirnics, K., and Pevsner, J. (2004). Progress in the use of microarray technology to study the neurobiology of disease. Nat. Neurosci. *7*, 434–439.

Nishimura, A.L., Mitne-Neto, M., Silva, H.C., Richieri-Costa, A., Middleton, S., Cascio, D., Kok, F., Oliveira, J.R., Gillingwater, T., Webb, J., et al. (2004). A mutation in the vesicle-trafficking protein VAPB causes late-onset spinal muscular atrophy and amyotrophic lateral sclerosis. Am. J. Hum. Genet. *75*, 822–831.

Pennetta, G., Hiesinger, P.R., Fabian-Fine, R., Meinertzhagen, I.A., and Bellen, H.J. (2002). Drosophila VAP-33A directs bouton formation at neuromuscular junctions in a dosage-dependent manner. Neuron *35*, 291–306.

Price, D.L., Tanzi, R.E., Borchelt, D.R., and Sisodia, S.S. (1998). Alzheimer's disease: genetic studies and transgenic models. Annu. Rev. Genet. *32*, 461–493.

Rizzu, P., Van Swieten, J.C., Joosse, M., Hasegawa, M., Stevens, M., Tibben, A., Niermeijer, M.F., Hillebrand, M., Ravid, R., Oostra, B.A., et al. (1999). High prevalence of mutations in the microtubule-associated protein tau in a population study of frontotemporal dementia in the Netherlands. Am. J. Hum. Genet. *64*, 414–421.

Robinow, S., and White, K. (1988). The locus elav of Drosophila melanogaster is expressed in neurons at all developmental stages. Dev. Biol. *126*, 294–303.

Rubin, G.M., and Spradling, A.C. (1982). Genetic transformation of Drosophila with transposable element vectors. Science *218*, 348–353.

Safavi, A., and Hersh, L.B. (1995). Degradation of dynorphin-related peptides by the puromycin-sensitive aminopeptidase and aminopeptidase M. J. Neurochem. *65*, 389–395.

Sang, T.K., Li, C., Liu, W., Rodriguez, A., Abrams, J.M., Zipursky, S.L., and Jackson, G.R. (2005). Inactivation of Drosophila Apaf-1 related killer suppresses formation of polyglutamine aggregates and blocks polyglutamine pathogenesis. Hum. Mol. Genet. *14*, 357–372.

Santacruz, K., Lewis, J., Spires, T., Paulson, J., Kotilinek, L., Ingelsson, M., Guimaraes, A., DeTure, M., Ramsden, M., McGowan, E., et al. (2005). Tau suppression in a neurodegenerative mouse model improves memory function. Science *309*, 476–481.

Schonlein, C., Loffler, J., and Huber, G. (1994). Purification and characterization of a novel metalloprotease from human brain with the ability to cleave substrates derived from the N-terminus of beta-amyloid protein. Biochem. Biophys. Res. Commun. *201*, 45–53.

Schulz, C., Perezgasga, L., and Fuller, M.T. (2001). Genetic analysis of dPsa, the Drosophila orthologue of puromycin-sensitive aminopeptidase, suggests redundancy of aminopeptidases. Dev. Genes Evol. *211*, 581–588.

Shen, Y., and Meri, S. (2003). Yin and Yang: complement activation and regulation in Alzheimer's disease. Prog. Neurobiol. *70*, 463–472.

Shulman, J.M., and Feany, M.B. (2003). Genetic modifiers of tauopathy in Drosophila. Genetics *165*, 1233–1242.

Sisodia, S.S., and St George-Hyslop, P.H. (2002). gamma-Secretase, Notch, Abeta and Alzheimer's disease: where do the presenilins fit in? Nat. Rev. Neurosci. *3*, 281–290.

Small, S.A., Kent, K., Pierce, A., Leung, C., Kang, M.S., Okada, H., Honig, L., Vonsattel, J.P., and Kim, T.W. (2005). Model-guided microarray implicates the retromer complex in Alzheimer's disease. Ann. Neurol. *58*, 909–919.

Smith, D.E., and Fisher, P.A. (1989). Interconversion of Drosophila nuclear lamin isoforms during oogenesis, early embryogenesis, and upon entry of cultured cells into mitosis. J. Cell Biol. *108*, 255–265.

Spradling, A.C., and Rubin, G.M. (1982). Transposition of cloned P elements into Drosophila germ line chromosomes. Science *218*, 341–347.

Talapatra, S., Wagner, J.D., and Thompson, C.B. (2002). Elongation factor-1 alpha is a selective regulator of growth factor withdrawal and ER stress-induced apoptosis. Cell Death Differ. *9*, 856–861.

Tham, A., Nordberg, A., Grissom, F.E., Carlsson-Skwirut, C., Viitanen, M., and Sara, V.R. (1993). Insulin-like growth factors and insulin-like growth factor binding proteins in cerebrospinal fluid and serum of patients with dementia of the Alzheimer type. J. Neural Transm. Park. Dis. Dement. Sect. *5*, 165–176.

Thibault, S.T., Singer, M.A., Miyazaki, W.Y., Milash, B., Dompe, N.A., Singh, C.M., Buchholz, R., Demsky, M., Fawcett, R., Francis-Lang, H.L., et al. (2004). A complementary transposon tool kit for Drosophila melanogaster using P and piggyBac. Nat. Genet. *36*, 283–287.

Tobler, A.R., Constam, D.B., Schmitt-Graff, A., Malipiero, U., Schlapbach, R., and Fontana, A. (1997). Cloning of the human puromycin-sensitive aminopeptidase and evidence for expression in neurons. J. Neurochem. *68*, 889–897.

Wang, J.Z., Grundke-Iqbal, I., and Iqbal, K. (1996). Glycosylation of microtubule-associated protein tau: an abnormal posttranslational modification in Alzheimer's disease. Nat. Med. *2*, 871–875.

Wilczak, N., de Vos, R.A., and De Keyser, J. (2003). Free insulin-like growth factor (IGF)-I and IGF binding proteins *2*, 5, and 6 in spinal motor neurons in amyotrophic lateral sclerosis. Lancet *361*, 1007–1011.

Zhang, Y., Chen, K., Tu, Y., and Wu, C. (2004). Distinct roles of two structurally closely related focal adhesion proteins, alpha-parvins and beta-parvins, in regulation of cell morphology and survival. J. Biol. Chem. *279*, 41695–41705.